Turbulent Pipe Flow Heat Transfer with a Simultaneous Chemical Reaction of Finite Rate

P. L. T. BRIAN

Massachusetts Institute of Technology, Cambridge, Massachusetts

The rate of heat transfer from a solid wall to a gas mixture can be substantially affected by rapid reversible homogeneous reactions occurring between components in the gaseous mixture. The thermal gradients cause gradients in the equilibrium gas concentrations and thus produce enthalpy fluxes due to counter diffusion of reactants and products. For energetic chemical reactions these enthalpy fluxes can increase the net rate of heat transfer many fold. Examples of this phenomenon include air dissociation effects upon the rate of heat transfer to re-entering missiles and satellites (*1, 7, 12, 14, 15, 17, 22*) and the very high heat transfer coefficients observed when heat is transferred to nitrogen tetroxide-nitrogen dioxide mixtures (*3, 8, 10, 11, 16, 18, 20*).

When the homogeneous reaction rate is large relative to rates of diffusion within the boundary layer, the temperature and composition profiles through the boundary layer will correspond approximately to local chemical equilibrium. In this case heat transfer rates can be predicted by correlations for physical heat transfer except that effective values of the thermal conductivity and the heat capacity of the gas mixture are used (*3, 8, 10, 11, 16, 18, 20*). The effective equilibrium thermal conductivity and heat capacity of a reacting gas mixture can be substantially greater than the thermal conductivity and heat capacity that the mixture would have if the chemical reactions were frozen. Furthermore these effective properties will generally show much greater variations with temperature than the corresponding properties for gaseous mixtures undergoing no chemical reactions, and the variations with temperature must be considered in order to accurately account for observed heat transfer rates with large temperature driving forces. If the homogeneous reaction rate is high enough to cause the chemical reaction to have a substantial effect upon the heat transfer rate but is not high enough to justify the assumption of local chemical equilibrium, the use of effective thermal properties appears not to be a fruitful approach for predicting the rate of heat transfer. In this case the effective properties would be found to vary with the boundary-layer thickness and thus with the gas flow rate past the solid wall. The effect of a simultaneous chemical reaction of finite rate upon turbulent heat transfer is similar in many respects to the effect upon heat conduction in a stagnant gas layer, which is discussed by Brokaw (*4*).

In a recent publication (*2*) a theoretical solution was presented for the effect of a simultaneous chemical reaction of finite rate upon the rate of heat transfer between a wall and a reacting gas mixture. The analysis was based upon a film-theory model. By limiting the analysis to the case of a very small temperature driving force the reaction kinetic equation was linearized, and thus the results were given general expression in terms of the partial derivatives of arbitrary reaction kinetic equations. Speculation was presented to suggest that the film-theory results would probably be good approximations to the solution for turbulent flow if the Lewis number is equal to unity, but this could not be substantiated by any theoretical or experimental evidence. Furthermore the film-theory results give no indication of how a turbulent flow solution might be affected by variations in the Lewis number.

The objective of the present work is to extend the ideas in reference *2* to a more realistic fluid mechanical model for turbulent flow. The linearization for small values of the temperature driving force will be maintained in order that the results may be given general expression without reference to a particular chemical reaction kinetic equation. Because of the increased complexity of the fluid mechanical model this work has been restricted to consideration of binary gas mixtures and to homogeneous chemical reactions; the film theory solution in reference *2* is more general in these respects.

THEORY

The gas to be considered is an ideal gas mixture of components A and V which undergo the single reversible homogeneous reaction

$$A \leftrightharpoons v\,V \tag{1}$$

The net rate of the homogeneous chemical reaction is an arbitrary function of temperature and of the mole fraction of component A at the particular pressure under consideration (the pressure is assumed to vary by a negligible amount throughout the flow field):

$$r = F(T, y) \tag{2}$$

The specific heats of components A and V are assumed to be equal and to be constant with temperature; thus the heat of reaction is independent of temperature.

The flow model is that of turbulent flow in a round pipe in which heat and mass transport are assumed to occur by molecular and eddy diffusion in parallel. The eddy diffusivity for mass diffusion was assumed to be equal to the eddy diffusivity for heat diffusion, and the eddy diffusivity function of Deissler (*6*) was used, except for a modification near the center of the pipe:

$$\mathcal{E}/\nu = n^2 u^+ x^+ \,(1 - e^{-n^2 u^+ x^+}) \quad \text{for } 0 \leq x^+ \leq 26 \tag{3a}$$

$$\mathcal{E}/\nu = \frac{z x^+}{2.777} \quad \text{for } x^+ > 26 \text{ and } z \geq 1/2 \tag{3b}$$

$$\mathcal{E}/\nu = \frac{(N_{Re}/8)\sqrt{f/2}}{2.777}\left[\frac{1}{2} + z\right] \quad \text{for } 0 \leq z \leq 1/2 \tag{3c}$$

The constant n in Equation (3*a*) was taken as 0.124 as given by Deissler. Equation (3*b*) was not used by Deissler as such, but it can be obtained by differentiating Deissler's Equation (21) and substituting the result into his Equation (4) if the shear stress is assumed to vary linearly with

radius and if molecular viscosity is neglected relative to eddy viscosity. When Equation (3*b*) is applied all the way to the center of the pipe, it yields a value of the eddy diffusivity which comes back to zero at the center line. This behavior is contrary to the known facts, but it is usually thought to have a negligible effect upon the heat transfer coefficient computed. Nevertheless, because the use of Equation (3*b*) all the way to the center of the pipe produced some temperature and concentration profiles which appeared unrealistic, it was decided that Equation (3*c*) would be used for values of z less than ½. Equation (3*c*) simply provides for the eddy diffusivity to vary linearly with the pipe radius from its maximum value at $z = ½$ to half of that maximum value at the pipe center line. This variation, while it is undoubtedly not exact, is thought to be much closer to the actual eddy diffusivity variation near the center of the pipe than that given by Equation (3*b*). The use of Equation (3*c*) did eliminate the unreasonable behavior of the temperature and concentration profiles at the center line, but the heat transfer rate was substantially the same as that obtained when Equation (3*b*) was applied to the pipe center line in a number of runs. Deissler's function was chosen to represent the eddy diffusivity of heat and mass becaue it produces results in excellent agreement (*6*) with mass transfer and heat transfer data in the range of Schmidt and Prandtl numbers from unity to 3,000 (although it is not a true analogy in that it was not derived from velocity profile measurements). The modification near the center of the pipe which was adopted here had a negligible effect upon results predicted for heat transfer to a nonreacting gas, as is seen in Figure 6.

In order to account for the effect of local convection upon the radial variation in the heat and mass fluxes the local molal flow velocity in the axial direction divided by the average molal velocity was assumed to obey the generalized velocity profile of Von Kármán (*21*):

$$u^+ \sqrt{f/2} = g = x^+ \sqrt{f/2} \quad \text{for } 0 \leq x^+ \leq 5 \qquad (4a)$$

$$u^+ \sqrt{f/2} = g = (5 \ln x^+ - 3.05) \sqrt{f/2} \quad \text{for } 5 \leq x^+ \leq 30 \qquad (4b)$$

$$u^+ \sqrt{f/2} = g = (2.5 \ln x^+ + 5.5) \sqrt{f/2} \text{ for } x^+ > 30 \qquad (4c)$$

Of course one could obtain the velocity profile by integrating Equations (3*a*), (3*b*), and (3*c*) after making an assumption about the ratio of the eddy diffusivities of heat and momentum (Deissler assumed them to be equal), but the resulting velocity profile (*6*) would differ very little from Von Kármán's, and available data would not readily distinguish the better one. It is believed that such a small change in the velocity profile used to account for local convection would have a negligible effect upon the final result, and so Von Kármán's profile was selected for simplicity. Equations (4*a*) and (4*b*) were also used to compute u^+ values for use in Equation (3*a*); this is slightly different from Deissler's procedure, but the difference is negligible. The use of Von Kármán's profile to represent the molal flow velocity profile is justified by the very small radial variations in temperature and in composition resulting from assumptions to be discussed subsequently. Friction factor values for use in Equations (3*a*) through (4*c*) were chosen by trial so that integration of the velocity profile would produce a value of $\mathcal{G}$ equal to unity at the pipe wall. The resulting values of f were 0.008054, 0.004484, and 0.002876 at Reynolds numbers of 10^4, 10^5, and 10^6, respectively.

Uniform Heat Flux—Steady State

The use of an eddy diffusivity to describe turbulent transport is of course a great simplification. Nevertheless the partial differential equations describing this system will generally involve two independent space variables, the axial and radial positions, even when conditions are steady with time. A number of previous investigators (*6, 13*) treating the problem of turbulent pipe flow heat transfer without chemical reactions have avoided the necessity of considering axial variations by making the simplification

$$q = q_w z \qquad (5)$$

and considering only variations in the radial direction in integrating the resulting differential equation. Equation (5) cannot be justified rigorously, but it can be justified approximately for the case of a uniform wall heat flux, independent of axial position, or for the case in which the wall temperature varies linearly with axial position. In either of these two situations there will be an entrance region in which temperature profiles are developed, after which the axial temperature gradient will become substantially independent of radial position and equal to the axial gradient in the average stream temperature and to the axial gradient in the wall temperature (*19*). In this later region Equation (5) would apply if the velocity profile were flat, and Equation (5) would be expected to be a good approximation for turbulent flow.

For the present problem of simultaneous heat transfer and chemical reaction it would seem appropriate to begin by simplifying the problem in a manner similar to that adopted by investigators studying heat transfer without chemical reactions. Thus it is proposed to reduce the problem to one involving ordinary differential equations with radial position as the only independent variable rather than to tackle the complete problem involving axial as well as radial variations. Consider then heat transfer situations involving either a uniform wall heat flux or a wall temperature varying linearly with axial position. For a system in which the chemical reaction rate is a linear function of temperature and composition, after an entrance transient which depends upon the feed conditions, it seems reasonable to assume that the axial gradients in temperature and composition will become constant:

$$\left(\frac{\partial T}{\partial L}\right)_z = \text{independent of } z \text{ and } L = \left(\frac{dT_o}{dL}\right) \qquad (6)$$

$$\left(\frac{\partial y}{\partial L}\right)_z = \text{independent of } z \text{ and } L = \left(\frac{dy_o}{dL}\right) \qquad (7)$$

Equations (6) and (7) are equivalent to assuming that a solution to the problem can be found in which both T and y are composed of a function of z added to a linear function of L. This would require however that the reaction rate have an axial gradient which is independent of z and L, and it can be shown that functions of this form will satisfy the partial differential equations [Equations (9*a*), (10*a*), and (13)] only if

$$\left(\frac{\partial r}{\partial L}\right)_z = 0 \qquad (8)$$

Equation (8) corresponds to the steady state reaction rate assumption introduced in the appendix of reference 2. It can best be appreciated by following a slug of fluid down the pipe. Assume that the gas was in chemical equilibrium before it entered the heated pipe. As the gas flows through the entrance region, temperature and concentration gradients in the radial direction will be developed. Focusing for convenience upon the relatively well-mixed gas in the turbulent core, the heat transfer to this gas and the depletion of component A from this gas will generally not exactly balance each other to maintain the bulk gas in chemical equilibrium. Thus as this gas moves down the pipe, it will depart from chemical equilibrium more and more un-

til finally the reaction rate in this bulk gas will build up to the point where it is just sufficient to account for the imbalance between the rising temperature and the falling concentration of species A. After this the reaction rate will remain substantially constant at this steady state value (steady state in the sense of the residence time of a slug of gas). A derivation which indicates approximately how far down the pipe this steady state region is achieved is presented in the Appendix.*

Small Temperature Driving Force

As in reference 2 this analysis will be limited to the case of a very small temperature difference between the wall and the pipe centerline. In the two physical situations discussed in the preceeding paragraphs this would correspond to a sufficiently low uniform wall heat flux, or to a wall temperature varying linearly with axial poition and with a sufficiently low slope so as to produce a very small temperature difference between the pipe wall and the gas in the center of the pipe. This small temperature driving force assumption limits the applicability of the results obtained, but it permits the linearization of the reaction rate equation and of the diffusion equation, thus allowing the results to be expressed quite generally without reference to a particular reaction kinetic equation.

Development of Equations

Effects such as the perturbation in the fluid mechanical parameters due to the diffusion fluxes and kinetic energy effects within the gas are assumed to be negligible. A material balance on component A yields

$$\frac{\partial(zN_A)}{\partial z} = \left(\frac{zd}{2}\right)\left[r + \frac{\partial(Ggy)}{\partial L}\right] \tag{9a}$$

$$= \left(\frac{zd}{2}\right)\left[r + \frac{\mathrm{Gg}\left(\frac{dy_o}{dL}\right)}{1+\theta y_o}\right] \tag{9b}$$

Equation (9b) is obtained from Equation (9a) by relating the axial variation in G to the axial variation in y by the reaction stoichiometry, by using Equation (7), and by assuming that radial variations in y are very small compared with unity because of the assumption of a very small temperature driving force. Similarly for component V

$$\frac{\partial(zN_V)}{\partial z} = \left(\frac{zd}{2}\right)\left[-vr + \frac{\partial(Gg(1-y))}{\partial L}\right] \tag{10a}$$

$$= \left(\frac{zd}{2}\right)\left[-vr - \frac{vgG\left(\frac{dy_o}{dL}\right)}{1+\theta y_o}\right] \tag{10b}$$

Equations (9b) and (10b) can be combined to give

$$\frac{\partial[z(N_V + vN_A)]}{\partial z} = 0 \tag{11}$$

which can be integrated to yield

$$N_V + vN_A = 0 \tag{12}$$

In integrating Equation (11) the constant of integration is found to be zero by considering the boundary condition at $z = 1$, where both fluxes are zero if there is no heterogeneous reaction. (Even if there is a heterogeneous reaction the stoichiometry of that reaction will require that the constant of integration must be zero.)

* Tabular material has been deposited as document 7723 with the American Documentation Institute, Photoduplication Service, Library of Congress, Washington 25, D. C., and may be obtained for $1.25 for photoprints or for 35-mm. microfilm.

The first law of thermodynamics applied to a differential control volume yields

$$\frac{\partial[z(q + N_AH_A + N_VH_V)]}{\partial z} = \left(\frac{zd}{2}\right)\left[\frac{\partial[Gg(yH_A + (1-y)H_V]}{\partial L}\right] \tag{13}$$

which can be reduced to the form

$$\frac{\partial[z(q - N_A\Delta H)]}{\partial z} = \left(\frac{zd}{2}\right)\left[\frac{-gG\Delta H\left(\frac{dy_o}{dL}\right)}{1+\theta y_o} + gGC_p\left(\frac{dT_o}{dL}\right)\right] \tag{14}$$

by using Equation (12), relating axial variations in G to axial variations in y by reaction stoichiometry, by again neglecting radial variations in y relative to unity, and by using Equations (6) and (7). The symbol C_p in Equation (14) denotes the mole fraction-weighted average of the molal heat capacities of pure components A and V; this is often called the *frozen heat capacity*, and it is equal to the heat capacity that the gas mixture would have if the chemical reaction did not take place. Equation (8) requires that

$$\frac{(dy_o/dL)}{(dT_o/dL)} = -F_T/F_y \tag{15}$$

which reduces Equation (14) to the form

$$\frac{\partial[z(q - N_A\Delta H)]}{\partial z} = \left(\frac{zd}{2}\right)gGC_p\left(\frac{dT_o}{dL}\right)\eta' \tag{16}$$

Integrating Equation (16) with respect to z one obtains

$$z(q - N_A\Delta H) = (d/4)\,\mathcal{G}GC_p\eta'\,(dT_o/dL) \tag{17}$$

or at $z = 1$

$$q_w = (d/4)\,GC_p\eta'\,(dT_o/dL) \tag{17a}$$

When one remembers Equation (6), Equation (17a) can be seen to be in the form of the first law of thermodynamics applied to the entire pipe cross section in which the effective heat capacity of the flowing gas stream is $(C_p\eta')$. This is a most interesting result because $(C_p\eta')$ is in fact the effective heat capacity of the gas stream when it remains in chemical equilibrium, but Equation (17a) is valid even if there is a large departure from chemical equilibrium. This interesting result is a consequence of Equation (8), which requires that the departure from chemical equilibrium, while not negligible, must be invariant with axial position.

Equations (17) and (17a) can be combined to yield

$$z(q - N_A\Delta H) = q_w\,\mathcal{G} \tag{18}$$

Combining Equations (9b), (14), and (17a) one gets

$$\frac{\partial(zq)}{\partial z} = \left(\frac{zd}{2}\right)(r\Delta H) + \frac{2gzq_w}{\eta'} \tag{19}$$

In this linearized analysis for a very small temperature driving force the homogeneous reaction rate is expanded as a linear function of temperature and composition:

$$r = r_o + F_T\,(T - T_o) + F_y\,(y - y_o) \tag{20}$$

The partial derivatives F_T and F_y could be evaluated most conveniently at T_E and y_E or at T_o and the composition in equilibrium with T_o. To do so would not make Equation (20) a poorer approximation than to evaluate the partial derivatives at T_o and y_o as long as r_o does not greatly ex-

ceed ($r_w - r_o$), and this does not occur in the results presented here. The radial fluxes of heat and mass are assumed to be given by equations in which molecular and eddy transport terms are additive:

$$q = \left(\frac{2k}{d}\right)\left[1 + N_{Pr}\left(\frac{\mathcal{E}}{\nu}\right)\right]\left(\frac{\partial T}{\partial z}\right) \quad (21)$$

$$N_A = \left(\frac{2\rho D}{d}\right)\left[1 + N_{Sc}\left(\frac{\mathcal{E}}{\nu}\right)\right]\left(\frac{\partial y}{\partial z}\right) + (N_A + N_V)y \quad (22a)$$

This can be combined with Equation (12) to yield

$$N_A = \left(\frac{2\rho\mathcal{D}}{d}\right)\left[1 + N_{Sc}\left(\frac{\mathcal{E}}{\nu}\right)\right]\left(\frac{\partial y}{\partial z}\right) \quad (22b)$$

Substitution of Equations (21) and (22b) into Equation (18) yields

$$\left(\frac{2k}{d}\right)\left[1 + N_{Pr}\left(\frac{\mathcal{E}}{\nu}\right)\right]\left(\frac{dT}{dz}\right) - \Delta H\left(\frac{2\rho\mathcal{D}}{d}\right)\left[1 + N_{Sc}\left(\frac{\mathcal{E}}{\nu}\right)\right]\left(\frac{dy}{dz}\right) = \frac{q_w\mathcal{G}}{z} \quad (23)$$

and substitution of Equations (20) and (21) into Equation (19) yields

$$\left(\frac{2k}{d}\right)\frac{d\left\{z[1 + N_{Pr}\,(\mathcal{E}/\nu)]\left(\frac{dT}{dz}\right)\right\}}{dz} = \left(\frac{zd}{2}\right)\Delta H\,[r_o + F_T(T - T_o) + F_y(y - y_o)] + \left(\frac{2gzq_w}{\eta'}\right) \quad (24)$$

In Equations (23) and (24) partial derivatives with respect to z have been replaced by ordinary derivatives because derivatives with respect to axial position do not appear in these equations; it is understood that they will be integrated with respect to z at a fixed axial position. It is convenient to express Equations (23) and (24) in terms of dimensionless variables:

$$\left(\frac{d\psi}{d\xi}\right) - F\left(\frac{d\sigma}{d\xi}\right) = \phi_c \quad (23a)$$

$$\mathcal{H}\frac{d\left[\mathcal{G}\left(\frac{d\psi}{d\xi}\right)\right]}{d\xi} = m[(\eta - 1)\,\psi + \sigma] + \epsilon\phi_c + \frac{4g\phi_c}{\eta'(N_{Nu_c}{}^*)} \quad (24a)$$

In these transformations the following equation was also used:

$$\frac{2}{(N_{Nu_c}{}^*)} = \int_o^1 \frac{\mathcal{G}\,dz'}{[z'][1 + N_{Pr}\,(\mathcal{E}/\nu)]} \quad (25)$$

Equation (25) can be verified by integrating Equation (23) for the special case in which ΔH is taken as zero. In Equation (25) ($N_{Nu_c}{}^*$) is the Nusselt number for heat transfer in the absence of a chemical reaction (or for a chemical reaction with ΔH = zero). It should be noted that this Nusselt number is defined in terms of a heat transfer coefficient based upon a center line temperature driving force ($T_w - T_o$). Furthermore ϕ_c, which appears in Equations (23a) and (24a), is the ratio of the heat transfer coefficient with chemical reaction to the heat transfer coefficient that would exist in the absence of a chemical reaction, both of these heat transfer coefficients being based upon the temperature difference between the wall and the center line of the pipe. The boundary conditions to be imposed upon the simultaneous solution of Equations (23a) and (24a) are

$$\text{At } \xi = 0 \begin{cases} \psi = 0 & (26a) \\ \sigma = 0 & (26b) \\ \mathcal{G}\left(\frac{d\psi}{d\xi}\right) = 0 & (26c) \end{cases}$$

$$\text{At } \xi = 1 \quad \psi = 1 \quad (26d)$$

These boundary conditions follow directly from the definitions of the dimensionless variables, with the exception that Equation (26c) requires in addition that the radial temperature gradient must be finite at the pipe center line. This temperature gradient could not be infinite unless the chemical reaction rate at the center line was infinite. One additional relation is needed regarding the mass diffusion flux at the pipe wall. For the case of no heterogeneous chemical reaction it is

$$\text{At } \xi = 1, \quad \frac{d\sigma}{d\xi} = 0 \quad (26e)$$

Equation (26e) can be used with Equation (23a) to yield

$$\phi_c = \left(\frac{d\psi}{d\xi}\right)_{\xi=1} \quad (27)$$

which can be used in place of Equation (26e).

Solution of the Equations

For selected values of the Reynolds number and the Prandtl number the integrand shown on the right-hand side of Equation (25) was integrated from the center line to various radial positions, yielding the Nusselt number for physical heat transfer according to Equation (25) and relating the transformed independent variable ξ to the radial position z. The integration was accomplished by use of the trapezoidal rule, employing the eddy diffusivity functions of Equations (3a), (3b), and (3c) with $\mathcal{G}$ being obtained by integration of the velocity profile functions of Equations (4a), (4b), and (4c). This transformation permits the functions $\mathcal{H}$, $\mathcal{G}$, and g to be uniquely related to the independent variable ξ. After a value of the Schmidt number is selected, the function F is also uniquely related to ξ, and Equations (23a) and (24a), subject to the boundary conditions of Equations (26a), (26b), (26c), (26d), and (27), can be solved for given values of m, η, and η'. These last two parameters cannot be chosen independently after the Prandtl number and the Schmidt number have been selected because they are related by the equation

$$\eta' - 1 = (\eta - 1)N_{Le} \quad (28)$$

The solution of these equations yields the radial profiles of temperature and composition (ψ, σ vs. ξ), the dimensionless steady state value of the chemical reaction rate at the center line ϵ, and the principal result desired here, ϕ_c, the ratio of the rate of heat transfer in the presence of the chemical reaction to the heat transfer rate which would be obtained in the absence of the chemical reaction at the same value of the temperature difference between the wall and the center line. The solution of these equations is not quite straightforward because ϕ_c, the desired answer, appears in the differential equations, Equations (23a) and (24a). A brief description of the method of solution used is presented in the Appendix.* The solution was accomplished by use of finite difference equations on an IBM-7090 digital computer.

* See footnote on page 833.

Bulk Temperature Driving Forces

In the variable transformations which produced Equations (23*a*) and (24*a*) the results were naturally and simply expressed in terms of ϕ_c and $N_{Nuc}{}^*$, which are defined in terms of heat transfer coefficients based upon the difference between the wall temperature and the center-line temperature. Results expressed in these terms are useful because of their simplicity, and they may be good approximations to results in turbulent boundary-layer flows for other geometrical configurations, such as flow past a submerged body. But for turbulent flow in a circular pipe the most convenient way to express the results is in terms of heat transfer coefficients based upon bulk temperature driving forces which are simply related to the average enthalpy of the flowing stream. For the case of heat transfer accompanied by a simultaneous chemical reaction several different kinds of bulk temperature driving forces can be suggested. For example the frozen mixing box temperature T_F is defined as the temperature that the flowing stream would achieve if the pipe were cut at the cross section in question and the stream were allowed to flow into an adiabatic mixing box in which no further chemical reaction took place. This frozen mixing box temperature can be computed by simply calculating the flow-weighted average temperature of the flowing stream. In terms of dimensionless variables this is accomplished by the following integration:

$$\frac{T_w - T_F}{T_w - T_o} = 1 - \int_o^1 g\,\psi\,2z'dz' \qquad (29)$$

On the other hand if the stream were allowed to flow into an adiabatic mixing box in which the system was brought to chemical equilibrium, the resulting temperature would be T_E, the equilibrium mixing box temperature. This temperature can be computed by the following equation in dimensionless form:

$$\frac{T_w - T_E}{T_w - T_o} = 1 - \frac{1}{\eta'}\left\{\int_o^1 g(\psi - \sigma N_{Le})2z'\,dz'\right\} + \left(\frac{\epsilon\,\phi_c}{m\,\eta'}\right)N_{Le} \qquad (30)$$

This equation is derived by first computing the frozen mixing box temperature and the frozen mixing box composition, then requiring that the equilibrium mixing box temperature and composition T_E and y_E be such that they give the same enthalpy as the frozen mixing box temperature and composition and in addition satisfy the equation

$$r_o + F_T(T_E - T_o) + F_y(y_E - y_o) = 0 \qquad (31)$$

which requires that they correspond to chemical equilibrium. Equation (31) is based upon the assumption that $(T_E - T_o)$ and $(y_E - y_o)$ are sufficiently small that the linearization of the reaction rate equation corresponding to Equation (20) is valid.

A third driving force which would appear to have considerable utility is one based upon enthalpy differences. Thus the difference between H'_w, the enthalpy that the gas mixture would have it it were brought to chemical equilibrium at the wall temperature and the system pressure, and $\overline{H'}$, the flow-weighted average enthalpy of the flowing stream, is a convenient driving force to use. For the case of a binary system H'_w is unambiguously defined in terms of the wall temperature T_w (although in multicomponent systems the definition might be ambiguous). Likewise $\overline{H'}$ is readily related to the amount of heat transfer which has taken place by the first law of thermodynamics. It is important that the driving force be based upon H', the enthalpy per unit mass, and not upon the enthalpy per mole of mixture for the general case in which θ is not equal to zero. It can be shown that the enthalpy driving force is simply related to the equilibrium mixing box temperature driving force by the factor η':

$$\frac{H'_w - \overline{H'}}{c_p(T_w - T_o)} = \eta'\left(\frac{T_w - T_E}{T_w - T_o}\right) \qquad (32)$$

For the case of heat transfer in the absence of chemical reaction the temperature profile is given by

$$\psi = \xi \qquad (33)$$

in terms of the dimensionless variables employed here. Thus the commonly used bulk temperature for the driving force for the heat transfer coefficient without chemical reaction can be obtained by an equation similar to Equation (29):

$$\left(\frac{T_w - T_B}{T_w - T_o}\right)^* = 1 - \int_o^1 g\xi\,2z'dz' \qquad (34)$$

Once Equations (23*a*) and (24*a*) have been solved to yield ϵ, ϕ_c, and the ψ and σ profiles, the integrals in Equations (29), (30), and (34) can be performed by use of the trapezoidal rule. Then the Nusselt number for heat transfer without chemical reaction but based upon a bulk driving force can be obtained by dividing $N_{Nuc}{}^*$ by the left-hand side of Equation (34). Similarly ϕ_F can be obtained by dividing ϕ_c by the ratio of the left-hand side of Equation (29) to the left-hand side of Equation (34). The value of ϕ_E, which is the ratio of the heat transfer coefficient with chemical reaction based upon an equilibrium mixing box temperature driving force to the heat transfer coefficient without chemical reaction based upon a bulk temperature driving force, can be obtained by dividing ϕ_c by the ratio of the left-hand side of Equation (30) to the left-hand side of Equation (34). Finally ϕ_H, which is the ratio of two heat transfer coefficients, that with chemical reaction to that without chemical reaction, both heat transfer coefficients being based upon an enthalpy driving force, is obtained simply by the relation

$$\phi_H = \phi_E/\eta' \qquad (35)$$

It is believed that ϕ_E and ϕ_H are more useful results than ϕ_F because they involve driving forces which are simply related to the average enthalpy of the flowing stream.

RESULTS AND DISCUSSION

Several criteria can be used to assess the accuracy of the computed results obtained in this study. First the manner in which the solution to the finite difference equations converges as the increment in the independent variable is decreased was used to assess the accuracy of the results. In addition the asymptotic value of ϕ as m approaches infinity is known, and the numerical results were compared with the known asymptotes. Finally if

$$\left.\begin{matrix} F = \mathcal{H} = \mathcal{G} = 1 \\ g = 0 \end{matrix}\right\} \quad \text{for } 0 \leq \xi \leq 1 \qquad (36)$$

this turbulent pipe flow model becomes synonomous with the film-theory model, and numerical solutions to Equations (23*a*) and (24*a*) with the functions as given by Equation (36) were compared with the analytical solution to the film theory given in reference 2 for a number of different sizes of the increment in the independent variable. The results of these comparisons lead the author to conclude that the ϕ values computed numerically in this study represent the true solution to Equations (23*a*) and (24*a*) within 2%, the error being less than 1% for most of the range of variables covered.

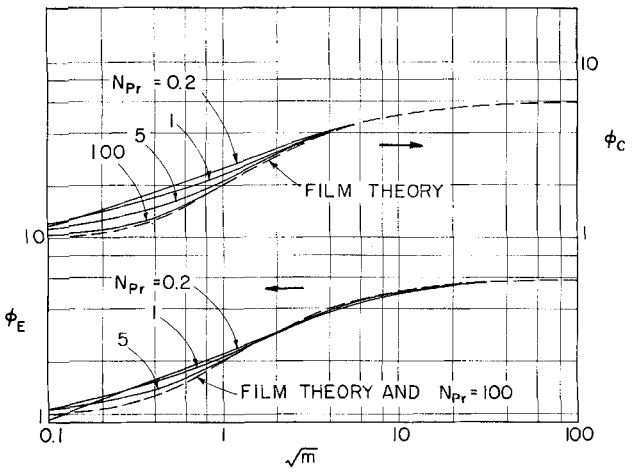

Fig. 1. Results for $N_{Re} = 10^6$, $N_{Le} = 1$, $\eta = \eta' = 6$.

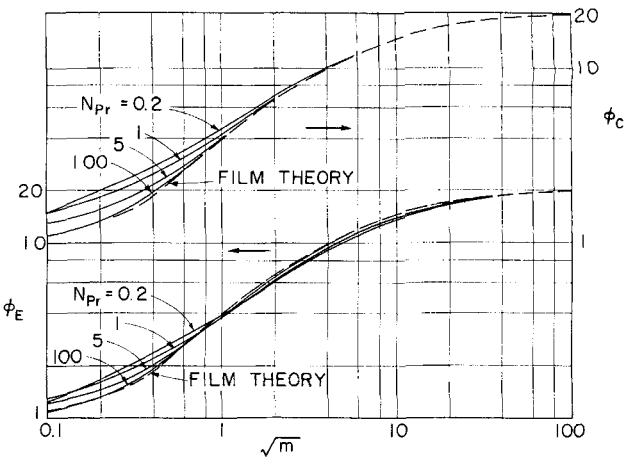

Fig. 3. Results for $N_{Re} = 10^6$, $N_{Le} = 1$, $\eta = \eta' = 21$.

Lewis Number Equal to Unity

When the Lewis number is equal to unity, η and η' are equal, and the asymptotic value of ϕ_c for an infinitely rapid reaction is known to be equal to η. For $\eta = 6$ the upper curves in Figure 1 present computed results for four different values of the Prandtl number at a Reynolds number of 10^6. These results are expressed as ϕ_c vs. $\sqrt{m}$ as in reference 2. This method of expressing the results is quite efficient, as will be seen later when the sensitivity of the curves to the Reynolds, Schmidt, and Prandtl numbers is examined. But while these plots display the effect of the chemical kinetic rate vividly, the effect of gas flow rate for example is not readily visualized because h^* appears in both ordinate and abscissa. A discussion of these effects and the relationship of this type of plot to the behavior of the physical system is presented in reference 2, where the analogy between this problem and the problem of gas absorption with simultaneous chemical reaction is indicated. The variable m is a measure of the chemical kinetic rate relative to diffusion rates within the boundary layer. For comparison the film-theory solution from reference 2 is shown also. The upper curves in Figures 2 and 3 present the same information for values of $\eta = 11$ and 21, respectively. Inspection of the ϕ_c curves in Figures 1 through 3 shows that, for a given value of η, the curves for the various Prandtl numbers approach each other and approach the film-theory solution rather closely for values of $\sqrt{m} > 2$ or 3. This suggests that the group m does a fair job of depicting the relative rate of the chemical reaction to the rate of diffusion and conduction within the boundary layer. Nevertheless curves for different values of the Prandtl number do deviate from each other at lower values of $\sqrt{m}$, the maximum deviation in Figure 3 being approximately 50% at a value of $\sqrt{m} = 0.2$. In the range of variables covered the value of ϕ_c is seen to increase with decreasing Prandtl number at a given value of $\sqrt{m}$, except for the crossover of the curves for Prandtl numbers of 0.2 and 1 at low values of $\sqrt{m}$. At $\sqrt{m} = 0.4$ results were obtained for Prandtl numbers lower than 0.2, and ϕ_c was observed to go through a maximum at a Prandtl number of approximately 0.2. Thus the effect of Prandtl number shown in Figures 1 through 3 should not be extrapolated to Prandtl numbers lower than 0.2.

The effect of Reynolds number on ϕ_c can be seen by comparing the upper curves in Figure 4 with those in Figure 2. At a Reynolds number of 10^4 the curves for the various values of the Prandtl number agree more closely with each other and with the film-theory solution than they do at a Reynolds number of 10^6. Results were also obtained at a Reynolds number of 10^5, and they were found to lie between those shown in Figure 2 and those in Figure 4.

It should be pointed out that ϕ_c does not approach unity as m approaches zero. This is in contrast to the film-theory solutions represented by Equation (36) of reference 2, which corresponds to a situation in which the bulk gas is at chemical equilibrium. On the other hand the simultaneous solution of Equations (A5) and (A14) in the appendix to reference 2 does not predict that ϕ approaches unity as m approaches zero if the film occupies an appreciable volume relative to the volume of the bulk

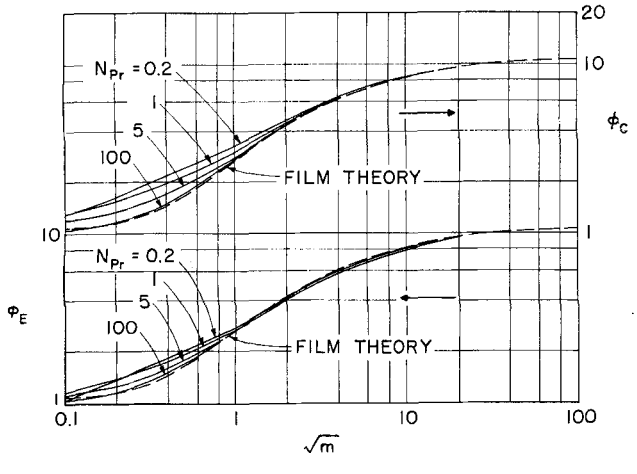

Fig. 2. Results for $N_{Re} = 10^6$, $N_{Le} = 1$, $\eta = \eta' = 11$.

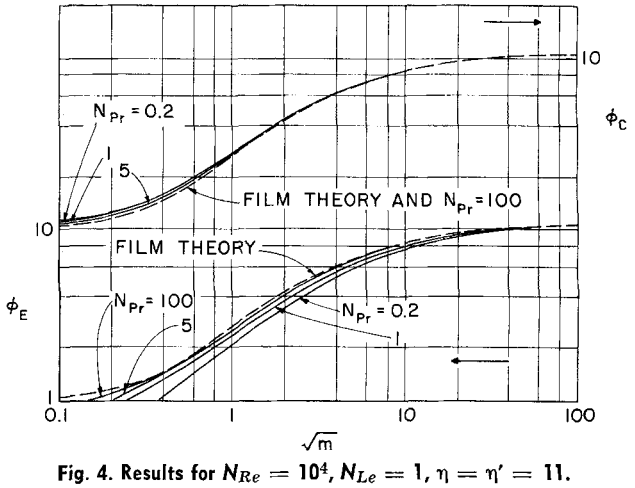

Fig. 4. Results for $N_{Re} = 10^4$, $N_{Le} = 1$, $\eta = \eta' = 11$.

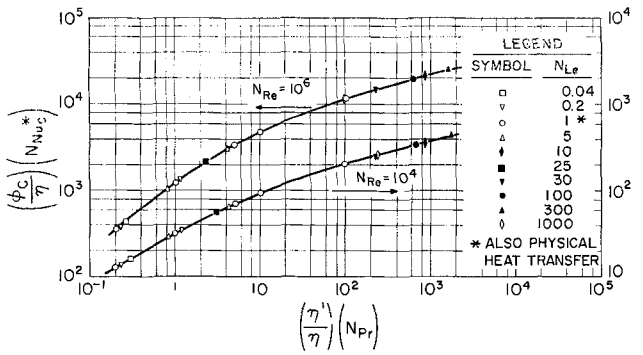

Fig. 5. Correlation for an infinitely rapid reaction $m = 10^6$.

gas. This is analogous to the present model, and the reason that the values of ϕ_c do not approach unity as m approaches zero is that the chemical reaction rate at the center line r_o is assumed in the present treatment to have built up to the value required to satisfy Equation (8), and this reaction rate increases q_w. As m approaches zero, this corresponds to a situation of little interest, and the steady state assumption has no utility at very low values of m, as will be discussed later.

The lower curves in Figures 1, 2, 3, and 4 present ϕ_E, which is based on the equilibrium mixing box temperature driving force. Values of ϕ_F were computed, but these results are omitted for brevity because ϕ_c, ϕ_E, and ϕ_H are believed to be the most useful results. At large values of m, ϕ_E and ϕ_F approach each other because local departures from chemical equilibrium decrease as m increases, and at very high values of m the stream would already be essentially in chemical equilibrium as it entered the mixing box. In addition when $N_{Le} = 1$, ϕ_E approaches ϕ_c at large values of m because the temperature profile approaches Equation (33), which is the temperature profile for physical heat transfer over most regions of the pipe, except for a thin region near the wall where there is a departure from chemical equilibrium. When one contrasts the lower curves with the upper curves in Figures 1, 2, and 3, it is seen that the values of ϕ_E are less sensitive to the Prandtl number for values of $\sqrt{m}$ between 0.1 and 1, but they are slightly more sensitive to the Prandtl number at values of $\sqrt{m}$ between 3 and 10. In addition at low values of $\sqrt{m}$, the curves for certain values of the Prandtl number cross each other several times.

In Figure 1 it can be seen that for a Prandtl number of 0.2, ϕ_E dips below unity at low values of $\sqrt{m}$. This effect is even more pronounced in Figure 4. Although the results are not shown, ϕ_E will continue to decrease without limit as m decreases. Inspection of Equation (30) reveals that the last term on the right-hand side approaches infinity as m approaches zero because ϵ is bounded as m tends to zero. Physically this means that the equilibrium mixing box temperature can depart from the wall temperature by an amount which is many fold greater than the difference between the wall temperature and the center-line temperature, this ratio approaching infinity in the limit as m tends toward zero. Again the reason for this behavior is the steady state assumption depicted by Equation (8). At very low values of m the reaction rate is insensitive to variations in composition and temperature and is thus essentially uniform across the pipe cross section, but nevertheless when the steady state region is reached, r_o must have built up to a sufficiently large value to satisfy Equation (15). Thus when the stream enters the equilibrium mixing box, very large changes in temperature and composition are required to bring it to equilibrium. Of course under these conditions the linearization of the reaction rate equation breaks down even though $(T_w - T_o)$ might be quite small. Thus in the steady state region the equilibrium mixing box temperature driving force is not useful at very low values of m.

Lewis Number Different from Unity

When the Lewis number is different from unity, ϕ_c does not approach η as m approaches infinity. However it is known (*3, 8, 10, 11, 16, 18, 20*) that as m approaches infinity the heat transfer coefficient will correlate with physical heat transfer results if effective equilibrium values of the thermal conductivity and the heat capacity of the reacting gas mixture are used. Thus a plot of $(\phi_c N_{Nuc}^*/\eta)$ vs. $(\eta' N_{Pr}/\eta)$ should correlate with physical heat transfer results plotted as N_{Nuc}^* vs. N_{Pr} for a given value of the Reynolds number. Figure 5 shows such a plot containing results for several different values of the Prandtl number and the Schmidt number. These results were all computed with $m = 10^6$, which corresponds essentially to an infinitely rapid chemical reaction. The points for cases in which the Lewis number is equal to unity are coincident with the physical heat transfer points because η, η' and ϕ_c are all equal when the Lewis number is equal to unity. It is clear from Figure 5 that the heat transfer results accompanied by an infinitely rapid chemical reaction do correlate with physical heat transfer results when the effective values of the thermal conductivity and of the heat capacity are used, thus confirming the accuracy of the computed results in this study for large values of m. Figure 6 shows a similar plot of $(\phi_E N_{NuB}^*/\eta)$ vs. $(\eta' N_{Pr}/\eta)$. The physical heat transfer points shown in Figure 6 agree well with those of Deissler (*6*) at a Reynolds number of 10^4, and the values at $N_{Re} = 10^6$ show satisfactory agreement with extrapolations of Deissler's values.

Since the asymptotic value of ϕ_c for a given value of η varies with both the Prandtl number and the Lewis number, it was decided that the most effective way to compare curves with different Schmidt numbers and different Prandtl numbers was to compare curves which are approaching the same asymptotic value of ϕ_c at large values of m, rather than compare runs with the same value of η. Figure 7 shows a plot of ϕ_c vs. $\sqrt{m}$ for several values of the Schmidt number and the Prandtl number centered around the values common for gases. For any combination of Schmidt number and Prandtl number the values of η and η' were chosen so that the asymptotic value of ϕ_c as given by Figure 5 would be 11 and so that Equation (28) would be satisfied. It should be noted that the curves in Figure 2 for values of the Prandtl number equal to 0.2, 1, and 5 fit logically in with the family of curves in Figure 7, but they were left off of Figure 7 for clarity. It can be seen in Figure 7 that, at values of $\sqrt{m}$ greater than 2, ϕ_c increases as the Lewis number decreases, and ϕ_c is relatively insensitive to the Prandtl number for a given value of the Lewis number. This later conclusion is also substan-

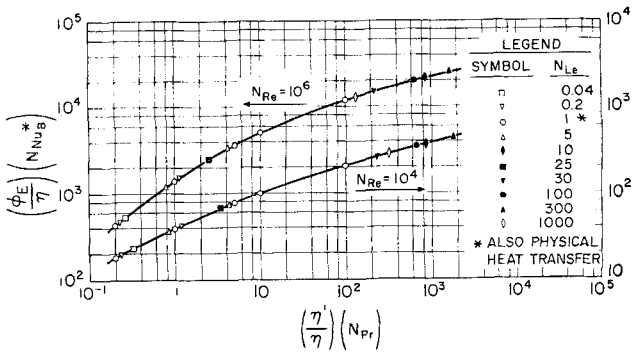

Fig. 6. Correlation for an infinitely rapid reaction $m = 10^6$.

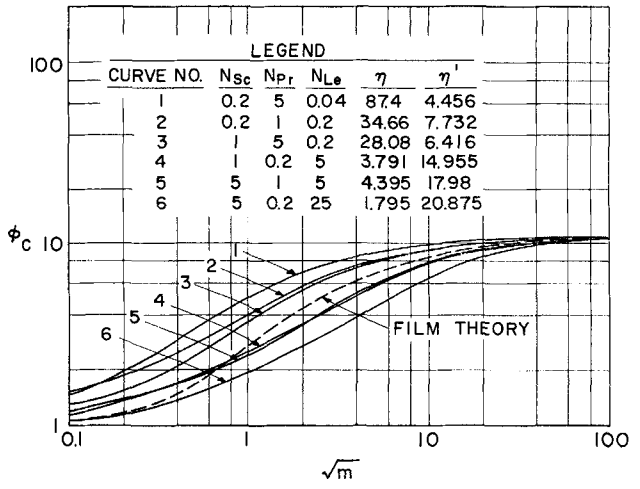

Fig. 7. Results for $N_{Re} = 10^6$, $N_{Le} \neq 1$.

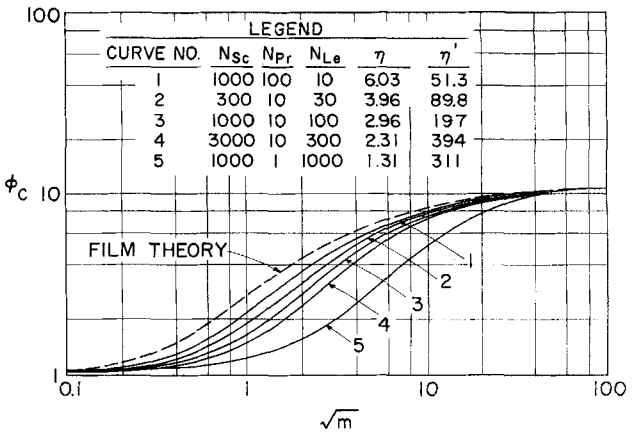

Fig. 9. Results for $N_{Re} = 10^6$, large Lewis number.

tiated for the case in which the Lewis number is equal to unity as shown in Figure 2, where it can also be seen that curves for $N_{Le} = 1$ closely approach the film-theory curve for $\eta = 11$. At values of $\sqrt{m} < 1$ the curves for different Prandtl numbers and the same number show deviations comparable in magnitude to the deviations shown in Figure 2 for a Lewis number equal to unity. All of the curves shown in Figure 7 converge at large values of $\sqrt{m}$ because the η' and η values for each curve were picked such that the asymptotic value of ϕ_c would be equal to 11.

Figure 8 shows a plot of ϕ_E vs. $\sqrt{m}$ for the same values of the Prandtl number and the Schmidt number which are shown in Figure 7. For any combination of the Prandtl number and the Schmidt number the values of η and η' have been selected such that the asymptotic value of ϕ_E as given in Figure 6 will be 11 and so that Equation (28) will be satisfied. Note that this produces slightly different values of η and η' from those shown in Figure 7 for the same values of the Prandtl number and the Schmidt number. This is because the asymptotic value of ϕ_E is not equal to the asymptotic value of ϕ_c for fixed values of the Prandtl number, the Schmidt number, η, and η'. As before, the results in Figure 2 for Prandtl numbers of 0.2, 1, and 5 fit into the family of curves shown in Figure 8. Figures 7 and 8 show that ϕ_E varies similarly to ϕ_c except at low values of $\sqrt{m}$.

For comparison with the results of Figures 7 and 8, Figures 9 and 10 present results for several values of the Prandtl number and the Schmidt number centered around common values for liquid systems. As before, the values of η and η' for each curve were picked so that the asymptotic value of ϕ at large values of m would be 11 for each curve. These results for large values of the Lewis number all lie below the film theory curve for $\eta = 11$, shown for comparison, and ϕ can be seen to decrease with an increase in the Schmidt number at constant Prandtl number or with a decrease in Prandtl number at constant Schmidt number. Thus ϕ decreases as the Lewis number increases.

Figures 11 through 14 present results at a Reynolds number of 10^4 and at Prandtl and Schmidt numbers corresponding to those in Figures 7 through 10. Comparison of these graphs reveals an effect of Reynolds number similar to that shown in Figures 2 and 4. The ϕ_c values at a given Lewis number are less sensitive to Prandtl number at the lower Reynolds number than at the higher Reynolds number, but the opposite is true of the ϕ_E values.

Rate of Approach to the Steady State Reaction Rate Condition

All of the results presented in this analysis are for a steady state region in which Equations (6), (7), and (8) are assumed to apply. At several points earlier in the discussion it was pointed out that this steady state condition is not a useful assumption at very low values of m. From a practical point of view it would be well to inquire into the rate at which the reaction rate would approach its steady state value as the gas flows down the pipe. Visualize the gas entering the pipe at chemical equilibrium. As it flows down the pipe the temperature and concentration profiles will be established, and the imbalance between heat transfer and mass transfer will cause the departure from chemical equilibrium at any radial position

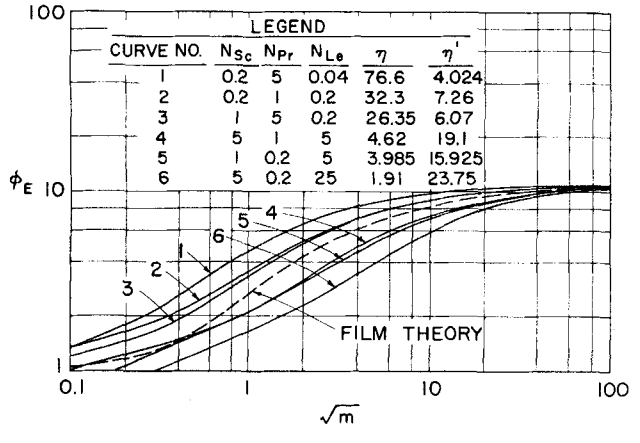

Fig. 8. Results for $N_{Re} = 10^6$, $N_{Le} \neq 1$.

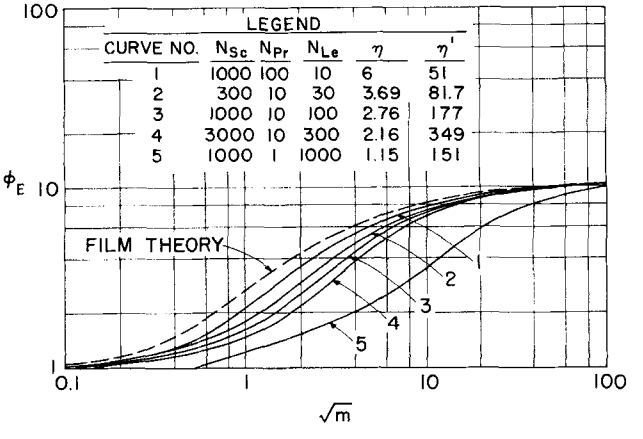

Fig. 10. Results for $N_{Re} = 10^6$, large Lewis number.

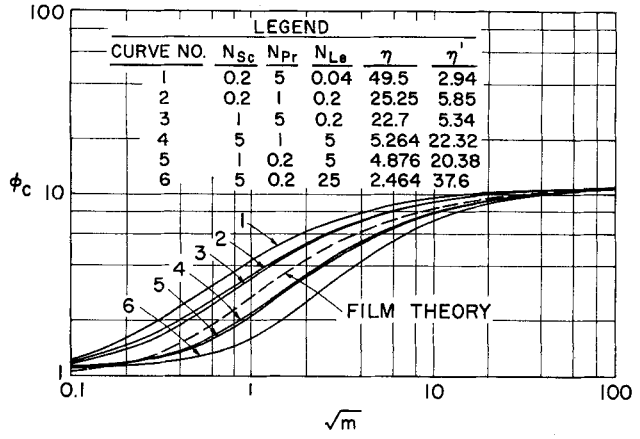

Fig. 11. Results for $N_{Re} = 10^4$, $N_{Le} \neq 1$.

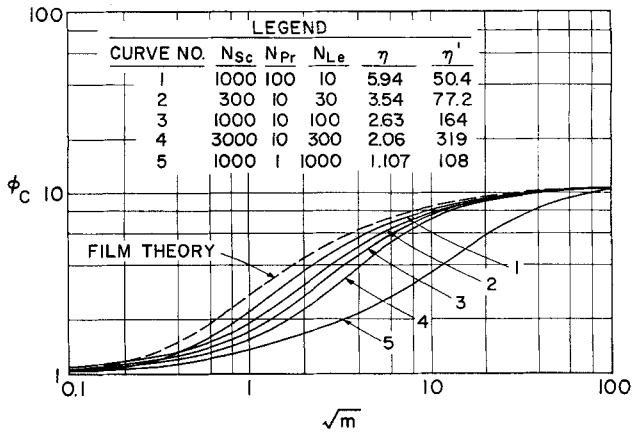

Fig. 13. Results for $N_{Re} = 10^4$, large Lewis number.

to build up and asymptotically approach its steady state value. An approximate analysis given in the Appendix* results in the following expression for the distance downstream at which the reaction rate will have built up exponentially to 99% of its steady state value

$$\left(\frac{L}{d}\right)_{99\%} = \frac{4.6\, N_{Re}\, N_{Sc}}{m\eta'\,(N_{Nu_C}{}^*)^2} \qquad (37)$$

The result is expressed in terms of the number of pipe diameters at which the reaction rate will be 99% of its steady state value, and this is seen to depend upon the Reynolds number, the Schmidt number, the Prandtl number, and η' and to be inversely proportional to the value of m. Thus at very low values of m the number of pipe diameters required to approach the steady state region would be so large that the steady state assumption adopted in the present analysis would not be generally useful.

As an example of the implications of Equation (37) consider Curve 5 in Figure 10. At $m = 0.25$ Equation (37) gives $(L/d)_{99\%} = 82$. For values of m less than 0.25 $(L/d)_{99\%}$ will be greater than 82, and the steady state assumption would not be applicable except to pipes with very large (L/d) ratios. Thus the region of the curve for which $\phi_E < 1$ is of limited interest, but this region is nevertheless attainable and might be of practical interest.

Multicomponent Systems

The results of this study are not generally applicable to multicomponent systems. However if all binary pair diffusion coefficients are equal, these results can be applied to a multicomponent system by using the definitions given in reference 2 for m, η, and η' for the special case of equal diffusivities.

Applicability of the Model

Equations (21) and (22a) represent a diffusion model of the turbulent mixing process which has proved to be quite useful as a means of attacking heat and mass transfer problems with nonreacting systems, and it seems logical to assume that the model will apply equally well to a reacting system. Nevertheless it should be recognized that this is an assumption which cannot be rigorously justified. Furthermore the use of time-mean values of T and y in evaluating $F(T, y)$ neglects the effect of the temperature and concentration fluctuations (5) on the chemical reaction rate. Thus it is clearly desirable that these predicted results should be confronted with experimental data.

It is encouraging that at large values of m the present results agree with experimental results for the nitrogen dioxide-nitrogen tetroxide system and with computations performed by replacing frozen k and C_p values with equilibrium values in the standard equations for nonreacting systems (*3, 8, 10, 11, 16, 18, 20*). Thus it may be expected that the present results would also apply to systems with intermediate values of m, but experiments are needed to confirm this. Such experiments are under way in the laboratory at Massachusetts Institute of Technology.

CONCLUSION

Results have been presented from numerical solutions for the effect of a reversible chemical reaction of finite

* See footnote on page 833.

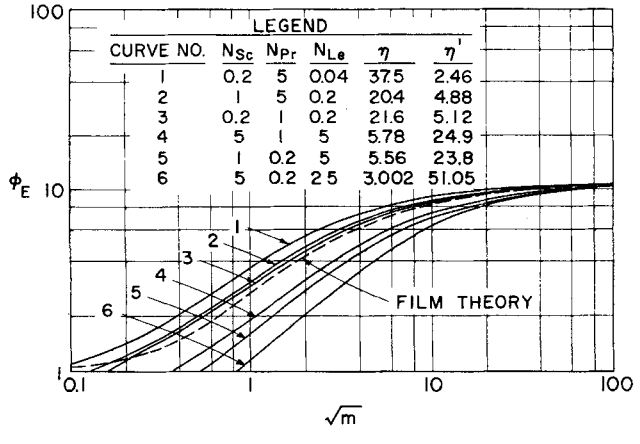

Fig. 12. Results for $N_{Re} = 10^4$, $N_{Le} \neq 1$.

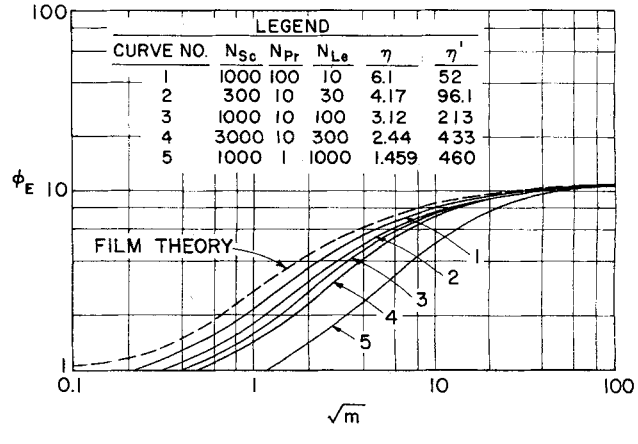

Fig. 14. Results for $N_{Re} = 10^4$, large Lewis number.

rate upon the rate of heat transfer in turbulent pipe flow. Linearization of the problem for a very small temperature driving force permits the expression of the results in terms of partial derivatives of an arbitrary reaction kinetic expression. The problem was simplified by focusing upon the steady state region in which the reaction rate is invariant with axial position at a given radial position, which will develop when the wall heat flux is constant with axial position. This steady state region is of no interest when the parameter m is very small, and values of m for which these results are not useful have been indicated by Equation (37).

The results show that the curve of ϕ vs. $\sqrt{m}$ for a given Lewis number is quite insensitive to Reynolds number and Prandtl number except at quite low values of $\sqrt{m}$ and low values of the Prandtl number. In the range of higher values of $m(\sqrt{m} > 2)$ the results for the Lewis number equal to unity agree well with film-theory results, and, at a given value of $\sqrt{m}$, ϕ decreases as the Lewis number increases.

ACKNOWLEDGMENT

The machine computations were performed at the Massachusetts Institute of Technology Computation Center. This work was initiated with financial support from an unrestricted grant from Socony Mobil Oil Company, and the work was completed with support from the National Science Foundation under Grant No. GP-537. Most of the numerical calculations were programmed and executed by Demetrios C. Matiatos. The author is indebted to Professors R. C. Reid and K. A. Smith for a number of stimulating discussions during the course of this work.

NOTATION

A = reactant in chemical reaction

C_p = frozen molal heat capacity at constant pressure, (B.t.u.)/(lb.mole)(°R.)

c_p = frozen specific heat (per unit mass) at constant pressure, (B.t.u.)/(lb.)(°R.)

$\mathcal{D}$ = $D/(1 + \theta y_o)$, (sq.ft./hr.)

D = binary diffusion coefficient for A-V mixture, (sq. ft./hr.)

d = pipe diameter, (ft.)

$\mathcal{E}$ = eddy diffusivity, (sq.ft./hr.)

e = 2.71828 . . . .

F = $(1 + N_{Pr}\ \mathcal{E}/\nu)/(1 + N_{Sc}\ \mathcal{E}/\nu)$

$F(T, y)$ = function of temperature and composition which expresses net rate of homogeneous reaction at fixed pressure under consideration, (lb. moles)/(hr.)(cu. ft.)

F_T = $\left(\frac{\partial F}{\partial T}\right)_y$, (lb. moles)/(hr.)(cu. ft.)(°R.), evaluated at T_E and y_E

F_y = $\left(\frac{\partial F}{\partial y}\right)_T$, (lb. moles)/(hr.)(cu. ft.) evaluated at T_E and y_E

f = Fanning friction factor

$\mathcal{G}$ = $\int_o^z 2z'g\,dz'$, fraction of molal flow in cylinder of radius $(zd/2)$

G = average molal flow velocity, (lb. moles)/(hr.)(sq. ft. pipe cross section)

g = local molal flow velocity divided by average molal flow velocity

$\mathcal{H}$ = $\mathcal{G}/z^2\,[1 + N_{Pr}\,(\mathcal{E}/\nu)]$

H = enthalpy per mole of a pure component, B.t.u./lb. mole

H' = enthalpy per pound of mixture, B.t.u./lb.

h = heat transfer coefficient in the presence of chemical reaction $q_w/\Delta T$, (B.t.u./hr.)(sq. ft.)(°R.); $h_c \equiv q_w/(T_w - T_o)$; $h_F \equiv q_w/(T_w - T_F)$; $h_E \equiv q_w/(T_w - T_E)$; $h_H \equiv c_p\,q_w/(H'_w - \overline{H'})$

h^* = physical heat transfer coefficient, that which would be found in the absence of chemical reaction, (B.t.u.)/(hr.)(sq. ft.)(°R.), $h_c^* \equiv q_w/(T_w - T_o)$; $h_B^* \equiv q_w/(T_w - T_B)$

k = frozen thermal conductivity of mixture, B.t.u./(hr.)(ft.)(°R.)

L = axial distance from pipe entrance, ft.

m = $F_y\,k^2/\rho\,\mathcal{D}(h_c^*)^2$

N_j = molal flux of component j in radial direction, lb. moles/(hr.)(sq.ft.), positive if directed toward pipe center line

n = constant in Equation (3a), equal to 0.124

N_{Le} = Lewis number $\equiv N_{Sc}/N_{Pr}$

N_{Nu} = Nusselt number $\equiv hd/k$; subscript and/or superscript denote which h it is based upon

N_{Pr} = frozen Prandtl number, $C_p\,\rho\nu/k$

N_{Re} = Reynolds number, $d\bar{u}/\nu$

N_{Sc} = Schmidt number, ν/D

q = radial heat flux by molecular and eddy conduction, (B.t.u.)/(hr.)(sq. ft.), positive if directed toward pipe center line

q_w = heat flux through pipe wall, B.t.u./(hr.)(sq. ft.)

r = net rate of homogeneous reaction, (moles of A reacted)/(hr.)(cu. ft.)

T = temperature (°R.); T_B = bulk temperature (without chemical reaction), Equation (34); T_E = equilibrium mixing box temperature; T_F = frozen mixing box temperature; T_o = center-line temperature; T_w = wall temperature

u = local axial flow velocity (time mean), ft./hr.

$\bar{u}$ = average axial velocity $\int_o^1 2z'\,u\,dz'$, ft./hr.

u^+ = $(u/\bar{u})\sqrt{2/f}$

V = product of chemical reaction

v = stoichiometric coefficient of species V

x = radial distance from wall toward pipe center line, ft.

x^+ = $\left(\frac{x}{d}\right) N_{Re}\sqrt{f/2}$

y = mole fraction of species A

z = reduced radial position $\equiv 1 - 2x/d$; z' when used as dummy variable in definite integral

Greek Letters

ΔH = enthalpy change of chemical reaction per mole of A reacted $\equiv vH_V - H_A$, B.t.u./(mole of A)

ϵ = $\Delta H\,r_o\,d/q_w\,N_{Nu_c}^*$

η = $1 + \dfrac{F_T\,\Delta H\,\rho\,\mathcal{D}}{F_y\,k}$, equilibrium thermal conductivity divided by frozen thermal conductivity

η' = $1 + \dfrac{F_T\,\Delta H}{F_y\,C_p(1 + \theta y_o)}$, equilibrium heat capacity divided frozen heat capacity

θ = $v - 1$, increase in moles due to reaction

ν = kinematic viscosity of fluid mixture, sq. ft./hr.

ξ = $\dfrac{\int_o^z \dfrac{\mathcal{G}\,dz'}{z'\,[1 + N_{Pr}(\mathcal{E}/\nu)]}}{\int_o^1 \dfrac{\mathcal{G}\,dz'}{z'\,[1 + N_{Pr}(\mathcal{E}/\nu)]}}$, dimensionless radial position

π = 3.14159 . . . .

ρ = molal density of mixture, (lb. moles total)/(cu. ft.)
σ = $(F_y/F_T)(\eta - 1)(y - y_o)/(T_w - T_o)$
ϕ_c = h_c/h_c^*
ϕ_E = h_E/h_B^*
ϕ_F = h_F/h_B^*
ϕ_H = h_H/h_B^*
ψ = $(T - T_o)/(T_w - T_o)$

Subscripts

A = species A
E = equilibrium mixing box conditions
i = pipe inlet
o = center line of pipe
ss = steady state, that is not changing with L
V = species V
w = pipe wall
99% = point at which ϵ is 99% of ϵ_{ss}

Superscripts

* = physical heat transfer

LITERATURE CITED

1. Altman, David, and Henry Wise, *J. Am. Rocket Soc.*, **26**, 256 (1956).
2. Brian, P. L. T., and R. C. Reid, *A.I.Ch.E. Journal*, **8**, 322 (1962).
3. Brokaw, R. S., *Natl. Advisory Comm. Aeronaut., Reclassification Notice, E57k19a* (March, 1958).
4. ———, *J. Chem. Phys.*, **35**, 1569 (1961).
5. Corrsin, Stanley, *Phys. Fluids*, **1**, 42 (1958).
6. Deissler, R. G., *Natl. Advisory Comm. Aeronaut. Rept. 1210* (1955). Reproduced in reference 9, pp. 253-280.
7. Fay, J. A., and F. R. Riddell, *J. Aeronaut. Sci.*, **25**, 73 (1958); *Res. Rept. No. 1*, Avco Corporation, Everett, Massachusetts (April, 1957).
8. Furguson, R. R., and J. M. Smith, *A.I.Ch.E. Journal*, **8**, 654 (1962).
9. Hartnett, J. P., ed., "Recent Advances in Heat and Mass Transfer," McGraw-Hill, New York (1961).
10. Irving, J. P., and J. M. Smith, *A.I.Ch.E. Journal*, **7**, 91 (1961).
11. Krieve, W. F., and D. M. Mason, *ibid.*, p. 277.
12. Lees, Lester, *Jet Propulsion*, **26**, 259 (1956).
13. Martinelli, R. C., *Trans. Am. Soc. Mech. Engrs.*, **69**, 947 (1947).
14. Metzdorf, H. J., *J. Aeronaut. Sci.*, **25**, 200 (1958).
15. Moore, L. I., *ibid.*, **19**, 505 (1952).
16. Richardson, J. L., F. P. Boynton, K. Y. Eng, and D. M. Mason, *Chem. Eng. Sci.*, **13**, 130 (1961).
17. Rose, P. H., R. F. Probstein, and M. C. Adams, *J. Aeronaut. Sci.*, **25**, 751 (1958).
18. Schotte, William, *Ind. Eng. Chem.*, **50**, 683 (1958).
19. Sleicher, C. A., Jr., and M. Tribus, *Trans. Am. Soc. Mech. Engrs.*, **79**, 789 (1957). Reproduced in reference 9, pp. 281-301.
20. Thievon, W. J., G. A. Sterbutzel, and J. L. Beal, *Wright Air Develop. Center. Tech. Rept. 59-450* (June, 1959).
21. Von Kármán, Theodore, *Trans. Am. Soc. Mech. Engrs.*, **61**, 705 (1939).
22. Ziebland, H., *J. Brit. Interplant. Soc.*, **14**, 249 (1955).

Manuscript received January 11, 1963; revision received July 8, 1963; paper accepted July 8, 1963. Paper presented at Heat Transfer Conference, Boston, Massachusetts (1963).

Calculation of Thermal Diffusion Factors for the Methane-n-Butane System in the Critical and Liquid Regions

W. M. RUTHERFORD

Mound Laboratory, Monsanto Research Corporation, Miamisburg, Ohio

Ordinary thermodynamic methods are inadequate for the treatment of steady state, nonequilibrium processes such as thermal diffusion. It is possible however to treat such phenomena by means of the thermodynamics of the steady state, the methods of which have been described by De Groot (*1*) and others (*2, 3*).

Steady state thermodynamic theory, as applied to the thermal diffusion phenomenon, gives a result for the thermal diffusion factor in terms of a single undetermined parameter, the heat of transport. The relationship between the thermal diffusion factor and the heat of transport may take several forms according to the particular choice of the form of the thermodynamic fluxes and forces used in the derivation. In a previous paper (*4*) the author has made use of the expression

$$\alpha = \frac{Q_1^{**}}{x_1(\partial\mu_1/\partial x_1)_{T,p}} \qquad (1)$$

where α is defined by the following equation for the mass flux of one component of a binary mixture subjected to a temperature gradient:

$$J_1 = \frac{D_{12}M_1\rho}{\bar{M}}\left[\nabla x_1 - \frac{\alpha x_1 x_2}{T}\nabla T\right] \qquad (2)$$

Q_1^{**} is the heat of transport and is the heat transported per mole of moving molecules of species 1 (in a two-component system) minus the enthalpy transport.

In reference *4* detailed experimental data were reported for thermal diffusion of methane-*n*-butane mixtures in the liquid and critical regions. These data were used to demonstrate the strong dependence of the thermal diffusion factor on the chemical potential derivative $(\partial\mu_1/\partial x_1)_{T,P}$. No attempt was made to interpret or estimate Q_1^{**}, although it was clear from the experimental results that Q_1^{**} is a function of temperature and pressure.

PREDICTION OF THE THERMAL DIFFUSION FACTOR

By another choice of thermodynamic fluxes and forces a different, but equivalent, expression for the thermal diffusion factor can be derived